A Microscopic Theory of the Neutron (I)

J.X. Zheng-Johansson

Institute of Fundamental Physics Research, 611 93 Nyköping, Sweden
January, 2015

Abstract.

A microscopic theory of the neutron, which consists in a neutron model constructed based on key relevant experimental observations, and the first principles solutions for the basic properties of the model neutron, is proposed within a framework consistent with the Standard Model. The neutron is composed of an electron e and a proton p that are separated at a distance $r_1 \sim 10^{-18}$ m, and are in relative orbital angular motion and Thomas precession highly relativistically, with their reduced mass moving along a quantised $l = 1$th circular orbit of radius r_1 about their instantaneous mass centre. The associated rotational energy flux or vortex has an angular momentum $\frac{1}{2}\hbar$ and is identifiable as a (confined) antineutrino. The particles e, p are attracted with one another predominantly by a central magnetic force produced as result of the particles' relative orbital, precessional and intrinsic angular motions. The interaction force (resembling the weak force), potential (resembling the Higgs' field), and a corresponding excitation Hamiltonian (H_I), among others, are derived based directly on first principles laws of electromagnetism, quantum mechanics and relativistic mechanics within a unified framework. In particular, the equation for $\frac{4}{3}\pi r_1^3 H_I$, which is directly comparable with the Fermi constant G_F, is predicted as $G_F = \frac{4}{3}\pi r_1^3 H_I = A_o C_{01}/\gamma_e\gamma_p$, where $A_o = e^2\hbar^2/12\pi\epsilon_0 m_e^0 m_p^0 c^2$, m_e^0, m_p^0 are the e, p rest masses, C_{01} is a geometric factor, and γ_e, γ_p are the Lorentz factors. Quantitative solution for a stationary meta-stable neutron is found to exist at the extremal point $r_{1m} = 2.513 \times 10^{-18}$ m, at which the G_F is a minimum (whence the neutron lifetime is a maximum) and is equal to the experimental value. Solutions for the neutron spin ($\frac{1}{2}$), apparent magnetic moment, and the intermediate vector boson masses are also given in this paper.

1. Introduction

The overall observational properties of the neutron, including the neutron spin, β decay reaction equation, parity, and Fermi constant, among others, are comprehensively summarised in the Standard Model (SM) for elementary particles [1]. The neutron β decay and a variety of similar so-termed weak phenomena, most notably the quantitative decay branching ratios in the decay processes, have been satisfactorily accounted for by the unified renormalisable theories of weak interaction. The Glashow-Weinberg-Salam (GWS) electroweak theory [2a-c] based on group $SU(2) \times U(1)$ is one of these. This theory in particular predicts the charged and neutral intermediate vector bosons W^-,W^+ and Z^0 which were confirmed by the experiments at CERN; its renormalisability was proven by t'Hooft in 1971 [2d]. All of the current field theories of the neutron are rested on the original hypothesis of Fermi [2e] that in a β decay reaction ($n \rightarrow p^+ + e^- + \bar{\nu}_e$), the matter particles $e^-, p^+, \bar{\nu}_e$ do not exist until the neutron n decays. And upon the neutron decay, these particles are envisaged as simply emitted by the neutron (as a point entity) in an analogous way to an accelerated point charge emitting electromagnetic radiation. The current theory of the neutron remains as a phenomenological one. There remain certain outstanding questions yet to be resolved. In particular, the origin of the weak interaction force is not well understood, an equation of the weak force accordingly is yet to be derived, and the Fermi constant (G_F) is not derived based on the interaction force. At a similar significant level, the nature and the origins of the (anti)neutrino, the intermediate vector bosons, the Weinberg weak mixing angle, and the Higgs mass are not yet fully well understood. One common feature suggestive of the

nature of the weak phenomena however is readily recognisable from observations, namely that the weak phenomena present only with the electrons and protons in the baryon (n, Λ, etc) and meson (π, K, etc.) disintegration processes, but not with the same electrons and protons in free-particle or bound atomic processes. For a more comprehensive understanding of the nature of the weak phenomena, a microscopic theory would be indispensable. The purpose of this paper is to propose a microscopic theory of the neutron based on a realistic real-space model construction of the neutron, serving as a prototype, such that the fundamental weak force and the variety of weak-interaction related properties and phenomena can be predicted based on first principles solutions in terms of the theory within a unified framework of electromagnetism, quantum mechanics, and special relativity.

Using several key relevant experimental facts, mainly the neutron beta decay reaction equation $n \rightarrow p + e + \bar{\nu}_e$, the neutron spin ($\frac{1}{2}$) and the order of magnitude of the Fermi constant G_F (which combined with the Heisenberg relation indicates a weak interaction distance of order $10^{-18}m$) as input information, we propose a real-space model of the neutron as follows: The *neutron* is composed of an electron e and a proton p separated at a distance $r(= r_1)$ of the order 10^{-18} m; see Fig 1a. The e, p are in relative orbital angular motions, and in addition relative Thomas precessions, at velocities approaching the velocity of light c under a central force of an electromagnetic origin. The central force is in effect predominantly an attractive magnetic force produced by the magnetic fields ($\mathbf{B}_e, \mathbf{B}_p$) resulting from the e, p intrinsic spin and relative motions. The z-components (S_{ez}, S_{pz}) of the e, p spin angular momenta are aligned parallel to each other and antiparallel to that of their relative motion ($Ł_{z,\text{-}1}$, Figs 1b), so that the magnetic interaction force is maximally attractive. The e, p relative motion is in such a way that their reduced mass ($\mathscr{M}$) moves at a velocity ($\boldsymbol{\upsilon}_1$) similarly approaching c along a (quantised $l = 1$th) circular orbit of radius $r(= r_1)$ about the common instantaneous centre of mass (CM) of e, p, with a normal ($\mathbf{n}$) at a precession-modified angle ($\pi - \theta_1$) to the z axis; see Fig 1b. The relative precessional–orbital angular momentum in z direction ($Ł_{z,\text{-}1}$) will show to be a half-integer quantum. The corresponding neutral rotational-energy-flux, or vortex, along the x, y

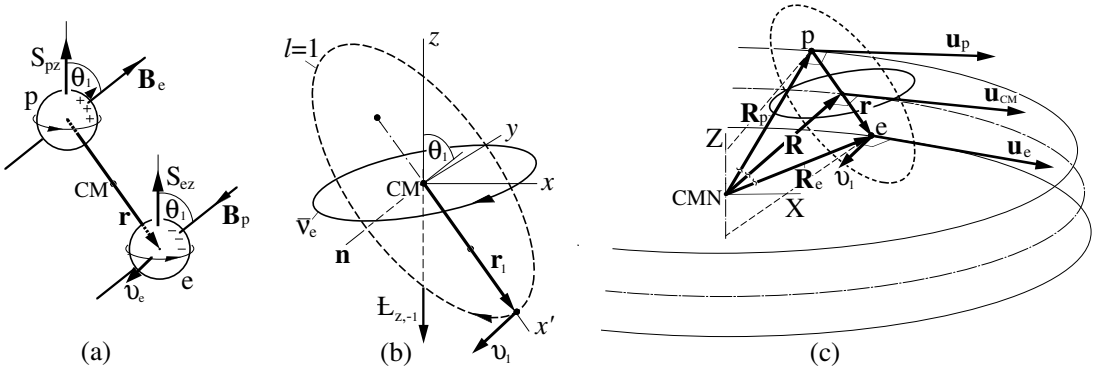

Figure 1. Schematic of the model neutron composed of an electron e and a proton p. (a) The e, p are separated by a distance $|\mathbf{r}| = |\mathbf{r}_1|$ and in relative angular motions and a Thomas precession; their spins are aligned in the z direction; (b) their reduced mass ($\mathscr{M}$) moves along a $l = 1$th orbit of radius r_1 about the CM. (c) The e, p relative angular motions are the differential results of their non-collinear total motions in circles of radii R_e, R_p about the CMN.

plane-projection of the $l = 1$th circular orbit, which conveys the angular momentum quantum $Ł_{z,\text{-}1}$, resembles a "confined" antineutrino ($\bar{\nu}_e$). Kinematically, the e, p relative angular motions are the result of their total motions in differing directions along circles of radii R_e, R_p about the centre of mass of the neutron (CMN), at velocities ($\mathbf{u}_e, \mathbf{u}_p$) similarly approaching c (Fig 1c).

It is commented that, the proposed e, p-neutron model has a built-in scheme for the strong force identically on a unified basis with electromagnetism: A proton p will be attracted with a neutron $n(e, p)$ (mainly) through a Coulomb attraction with the electron e of the neutron at short

range; at the same order of the short-range Coulomb interaction, two protons will repel, but never attract with one another. These characteristics are in accordance with the observational fact that no nucleus made of more than one protons, and only protons without neutrons, exists. Within this scheme, the observationally-never-isolatable quarks may be compared with the different modes of spins.

The remainder of this paper, I, gives a first-principles mathematical representation of the model neutron, mainly in respect to the internal relativistic kinematics, dynamics, and magnetic structure of the neutron in stationary state (Secs 2, 3), the dynamics upon the neutron β decay (Secs 4) and the quantitative determination of the dynamical variables (Sec 5). The (quantitative) predictions of the basic properties of the neutron given in this and separate papers are subsequently subjected to comparisons with, or constraints by the available experimental data where in question, so that a critical check of the viability of the neutron model is made. Other basic aspects regarding the neutron including parity associated with the β decay and direct derivations of the intermediate vector boson masses and Weinberg mixing angle, and a corresponding dynamic scheme for the other elementary particles participating weak processes, will be elucidated in separate papers (II, III).

2. Equations of motion. Coordinate transformations. Solutions

2.1. Transformed Newtonian equations of motion of the mean and instantaneous positions Consider that an electron e and a proton p comprising a neutron are at time t located with the probability densities $|\psi_\alpha(\mathbf{R}_\alpha, t)|^2$ ($\alpha = e, p$) at positions $\mathbf{R}_e, \mathbf{R}_p$ relative to the CMN; see Fig 1c. (The usual statistical point-particle picture is referred to here.) The observation is made in the instantaneous CM frame moving relative to the CMN; and the clock used to measure the time t is fixed at the CM. The particles e, p are in motions at velocities to prove high compared to c (Sec 5), under a mutual interaction force $\mathbf{F}$ and gravity $\mathbf{g}$; no applied force presents. Their mean positions, $\bar{\mathbf{R}}_\alpha = \int \mathbf{R}_\alpha |\psi_\alpha|^2 d^3R_\alpha$, evolve according to the transformed Newtonian equations of motion $\frac{d(m_\alpha(d\bar{\mathbf{R}}_\alpha/dt))}{dt} = \int (m_\alpha \mathbf{g} \pm \mathbf{F})|\psi_\alpha|^2 d^3R_\alpha$ (the correspondence principle), where m_e, m_p are the e, p masses. The e, p are assumed to form a bound stationary system until Sec 4 and hence necessarily move circularly at constant tangential velocities $\mathbf{u}_\alpha = d\mathbf{R}_\alpha/dt$ about the CMN (cf Fig 1c; Secs 2.3,2.5). The equations of motion thus reduce to

$$m_e \frac{d^2\mathbf{R}_e}{dt^2} = m_e \mathbf{g} + \mathbf{F}, \quad m_p \frac{d^2\mathbf{R}_p}{dt^2} = m_p \mathbf{g} - \mathbf{F}. \quad \text{Or} \quad M \frac{d^2\mathbf{R}}{dt^2} = M\mathbf{g}, \quad \mathscr{M} \frac{d^2\mathbf{r}}{dt^2} = \mathbf{F}, \tag{1}$$

$$\text{where } \mathbf{R} = \frac{m_e \mathbf{R}_e + m_p \mathbf{R}_p}{M}, \quad M = m_e + m_p, \quad \mathbf{r} = \mathbf{R}_e - \mathbf{R}_p = \mathbf{r}_e - \mathbf{r}_p, \quad \mathscr{M} = \frac{m_e m_p}{M};$$

$$\mathbf{R}_e = \mathbf{R} + \frac{m_p}{M}\mathbf{r}, \quad \mathbf{R}_p = \mathbf{R} - \frac{m_e}{M}\mathbf{r}; \quad \mathbf{r}_e = \mathbf{R}_e - \mathbf{R} = \frac{m_p}{M}\mathbf{r}, \quad \mathbf{r}_p = \mathbf{R}_p - \mathbf{R} = -\frac{m_e}{M}\mathbf{r}. \tag{2}$$

M is the total mass (at $\mathbf{R}$); $\mathbf{R}$ is the position of the CM (Fig 1c); $\mathscr{M}$ is the reduced mass and is alternatively expressible as $\frac{1}{\mathscr{M}} = \frac{1}{m_e} + \frac{1}{m_p}$; $\mathbf{r}$ is the relative position (Fig 1b); and $\mathbf{r}_e, \mathbf{r}_p$ are the e, p positions relative to $\mathbf{R}$. Eqs (1c) are given for the M and $\mathscr{M}$ travelling (circularly) at constant velocities $\mathbf{u}_{\rm cm} = d\mathbf{R}/dt$ (about the CMN), and $\boldsymbol{v} = d\mathbf{r}/dt$ (e relative to p), which are similarly necessary for a stationary bound e, p system.

The partial–relative and relative velocities of e, p, and the corresponding rotational angular momenta, follow as, given in terms of the time t,

$$\boldsymbol{v}_e = \frac{d\mathbf{r}_e}{dt} = \frac{m_p}{M}\boldsymbol{v}, \quad \boldsymbol{v}_p = \frac{d\mathbf{r}_p}{dt} = -\frac{m_e}{M}\boldsymbol{v}, \quad \boldsymbol{v}_e - \boldsymbol{v}_p = \boldsymbol{v} = \frac{d\mathbf{r}}{dt};$$

$$\mathbf{L}_e = \mathbf{r}_e \times (m_e \boldsymbol{v}_e) = \frac{m_p}{M}\mathbf{L}, \quad \mathbf{L}_p = \mathbf{r}_p \times (m_p \boldsymbol{v}_p) = \frac{m_e}{M}\mathbf{L}, \quad \mathbf{L} = \mathbf{L}_e + \mathbf{L}_e = \mathbf{r} \times (\mathscr{M}\boldsymbol{v}) \tag{4}$$

From (2g,h) it follows that the local times t_e, t_p measured by clocks fixed to the moving e, p are

related to t as $t_e = (m_p/M)t$, $t_p = (m_e/M)t$. The partial-relative velocities given in terms of t_e, t_p are $\boldsymbol{v}'_e = d\mathbf{r}_e/dt_e = \boldsymbol{v}$, $\boldsymbol{v}'_p = d\mathbf{r}_p/dt_p = -\boldsymbol{v}$.

2.2. Lorentz-Einstein transformations The instantaneous rest frame fixed to each rotating particle ($e, p, \mathscr{M}$ or M) may be regarded as an inertial frame for each differential rotation which is essentially linear. The non-inertial frame effect of a full rotation will be included separately (see Eqs 5h,i; Sec 2.5). Subsequently, the differentials of the space and time coordinates $\mathbf{r}_e$,$\mathbf{r}_p$,$\mathbf{R}$,$\mathbf{r}$,t in the CM frame and their counterparts $\mathbf{r}^0_e, \mathbf{r}^0_p, \mathbf{R}^0, \mathbf{r}^0, t^0$ in the respective (instantaneous) rest frames, and in turn $\mathbf{R}_e, \mathbf{R}_p, \mathbf{R}, t$ in the CM frame and $\mathbf{R}^L_e, \mathbf{R}^L_p$, $\mathbf{R}^L$, t^L in the Lab frame, are related by the Lorentz-Einstein transformations,

$$\gamma_e(d\mathbf{r}_e - \boldsymbol{v}_e dt) = d\mathbf{r}^0_e, \quad \gamma_p(d\mathbf{r}_p - \boldsymbol{v}_p dt) = d\mathbf{r}^0_p, \quad \gamma_{\rm cm}(d\mathbf{R} - \mathbf{u}_{\rm cm} dt) = d\mathbf{R}^0,$$
$$\gamma(d\mathbf{r} - \boldsymbol{v}dt) = d\mathbf{r}^0, \quad \gamma(dt - \boldsymbol{v}\cdot d\mathbf{r}/c^2) = dt^0; \quad \gamma^{L\prime}_{\rm cm}(d\mathbf{R}^L_e - \mathbf{u}^{L\prime}_{\rm cm} dt^L) = d\mathbf{R}_e,$$
$$\gamma^{L\prime\prime}_{\rm cm}(d\mathbf{R}^L_p - \mathbf{u}^{L\prime\prime}_{\rm cm} dt^L) = d\mathbf{R}_p, \quad \gamma^L_{\rm cm}(d\mathbf{R}^L - \mathbf{u}^L_{\rm cm} dt^L) = d\mathbf{R}^0, \quad \gamma^L_{\rm cm}(dt^L - \mathbf{u}^L_{\rm cm}\cdot d\mathbf{R}^L/{c^L}^2) = dt \quad (5)$$

where $\gamma_e = (1 - v_e^2/c^2)^{-1/2}$, $\gamma_p = (1 - v_p^2/c^2)^{-1/2}$, $\gamma_{\rm cm} = (1 - u^2_{\rm cm}/c^2)^{-1/2}$, $\gamma = (1 - v^2/c^2)^{-1/2}$, $c = d\mathbf{r}_{light}/dt$; $\mathbf{u}^L_{\rm cm} = d\mathbf{R}^L/dt^L$, $\gamma^L_{\rm cm} = (1 - {u^L_{\rm cm}}^2/{c^L}^2)^{-1/2}$, and $c^L (= d\mathbf{R}^L_{light}/dt^L)$ is the light speed measured in the Lab frame. $\gamma^{L\prime}_{\rm cm}$,$\gamma^{L\prime\prime}_{\rm cm}$ are the Lorentz factors associated with the CM-frame velocities at $\mathbf{R}^L_e, \mathbf{R}^L_p$, e.g. $\mathbf{u}^{L\prime}_{\rm cm} = d(\mathbf{R}^L_e - (m^L_p/M^L)\mathbf{r}^L)/dt^L$, which in general differ from $\gamma^L_{\rm cm}$ and $\mathbf{u}^L_{\rm cm}$ as the CM frame is in rotational, hence non-uniform motion. The CMN has been assumed at rest in the Lab frame.

Transformations from the scalar distances r_e, r_p, R, r to r^0_e, r^0_p, R^0, r^0 at fixed t, from the time t to t^0 at fixed $\mathbf{r}$, from the CM-frame masses $m_e, m_p, M, \mathscr{M}$ to the respective rest-frame counterparts $m^0_e, m^0_p, M^0 (= m^0_e + m^0_p), \mathscr{M}^0 (= m^0_e m^0_p/M^0)$, and further from a few involved CM-frame variables, with no suffixes, to the Lab-frame ones, suffixed by a superscript L, follow as

$$\gamma_e r_e = r^0_e, \quad \gamma_p r_p = r^0_p, \quad \gamma_{\rm cm} R = R^0, \quad \gamma r = r^0, \quad \gamma t = t^0; \quad m_e = \gamma_e m^0_e, \quad m_p = \gamma_p m^0_p, \quad (6.1)$$
$$M = \gamma_{\rm cm} M^0, \quad \mathscr{M} = \gamma \mathscr{M}^0; \quad \gamma^L_{\rm cm} R^L = R^0, \quad \gamma^L_{\rm cm} t^L = t, \quad M^L = \gamma^L_{\rm cm} M^0; \quad (6.2)$$
$$m^L_e = \gamma^{L\prime}_{\rm cm} m_e, \quad m^L_p = \gamma^{L\prime\prime}_{\rm cm} m_p; \quad \gamma^L_{{\rm cm},r} r^L = ((x - u_{\rm cm} t)^2 + z^2)^{1/2}, \quad \mathscr{M}^L = \gamma^L_{{\rm cm},r} \mathscr{M} \quad (6.3)$$

where $\gamma^L_{{\rm cm},r}$ is the r-projection of a Lorentz factor due to the motion of the CM frame in the direction $\mathbf{u}_{\rm cm}$. If $\gamma_e, \gamma_p > (>>)1$, then $\gamma_{\rm cm} > (>>)1$ based on (6.1f,g), (6.2a). This and Eqs (6.2a),(6.1c) suggest that $M \neq M^0$, $R \neq R^0$; i.e. M, R are not the proper rest total-mass and rest coordinate in the CM frame. Based on (2b), M is the sum of the e, p masses that are moving relative to the CM, not at rest. However, the CM is not moving relative to itself; all its relativistic effect results from its motion relative to the Lab frame at the velocity $\mathbf{u}_{\rm cm} = -\mathbf{u}^L_{\rm cm}$. We need therefore to imagine to fix to the Lab frame the proper M^0 and $\mathbf{R}^0$, which are now moving with it against the CM frame. It hence follows at once that $\gamma_{\rm cm} = \gamma^L_{\rm cm}$, $R = R^L$, $M = M^L$.

Using (6) for $m_e, m_p, M, \mathscr{M}$ in (2b),(d) gives (7), and solving gives (8):

$$\gamma_{\rm cm} M^0 = \gamma_e m^0_e + \gamma_p m^0_p, \quad \gamma_{\rm cm}\gamma = \gamma_e\gamma_p; \quad \text{or} \quad M^0 = m^\dagger_e + m^\dagger_p, \quad \text{where} \quad m^\dagger_e = \frac{m_e}{\gamma_{\rm cm}} = \gamma^\dagger_e m^0_e,$$
$$m^\dagger_p = \frac{m_p}{\gamma_{\rm cm}} = \gamma^\dagger_p m^0_p, \quad \gamma^\dagger_e = \frac{\gamma_e}{\gamma_{\rm cm}}, \quad \gamma^\dagger_p = \frac{\gamma_p}{\gamma_{\rm cm}}; \quad \gamma^\dagger_e\gamma^\dagger_p = \frac{\gamma_e\gamma_p}{{\gamma_{\rm cm}}^2} = \frac{\gamma}{\gamma_{\rm cm}} = \gamma^\dagger; \quad (7)$$
$$\gamma_e = \frac{\gamma_{\rm cm}(M^0 \pm \Gamma)}{2m^0_e}, \quad \gamma_p = \frac{\gamma_{\rm cm}(M^0 \pm \Gamma)}{2m^0_p}, \quad \Gamma = \sqrt{(M^0)^2 - 4m^0_e m^0_p \gamma^\dagger}. \quad (8)$$

For (8) to have real solutions requires $(M^0)^2 - 4m^0_e m^0_p \gamma^\dagger \geq 0$, or $\gamma^\dagger \leq \gamma^\dagger_{\rm max} = (M^0)^2/4m^0_e m^0_p = 459.536$, where $\gamma^\dagger = \gamma^\dagger_{\rm max}$ if $\Gamma = 0$, a special case of the e, p system with $\gamma_e, \gamma_p, \gamma_{\rm cm} >> 1$. For $\Gamma = 0$, (8a),(b) reduce to $\gamma_e = \gamma_{\rm cm} M^0/2m^0_e$, $\gamma_p = \gamma_{\rm cm} M^0/2m^0_p \simeq \frac{1}{2}\gamma_{\rm cm}$. These further give $m_e = m_p$, which relation may be judged to hold approximately for a realistic (model) neutron based on the resultant neutron g factor (Sec 2.6); Eqs (2g),(h) and (4a),(b) for this case become $\mathbf{r}_e = \frac{1}{2}\mathbf{r}$, $\mathbf{r}_p = -\frac{1}{2}\mathbf{r}$ and $\boldsymbol{v}_e = \frac{1}{2}\boldsymbol{v}$, $\boldsymbol{v}_p = -\frac{1}{2}\boldsymbol{v}$.

It is clear from Eq (7b), or $\gamma_e\gamma_p = \gamma_{\rm cm}^2\gamma^\dagger$, that the (proper) Lorentz factors γ_e, γ_p contain each a $\gamma_{\rm cm}$ associated with the motion of the CM-frame. The $\gamma_e^\dagger, \gamma_p^\dagger$ (which may be < 1) given after dividing $\gamma_{\rm cm}$ out in (7f),(g) represent "reduced" Lorentz factors expressed with reference to the proper M^0 in the CM frame. Mainly for formality, the corresponding dagger-suffixed quantities of $\mathbf{r}_e, \mathbf{r}_p, \mathbf{r}$, $t, \mathscr{M}$ are written down as, with (7) for $\gamma_e, \gamma_p, \gamma$ in Eqs (6.1a,b,d), (2g,h,c), (6.1e),(6.2b),

$$\gamma_{\rm cm}\mathbf{r}_e = \frac{\mathbf{r}_e^0}{\gamma_e^\dagger} = \mathbf{r}_e^\dagger = \frac{m_p^0}{M^0}\frac{\mathbf{r}^0}{\gamma_e^\dagger} = \frac{m_p^\dagger}{M^0}\mathbf{r}^\dagger, \quad \gamma_{\rm cm}\mathbf{r}_p = \frac{\mathbf{r}_p^0}{\gamma_p^\dagger} = \mathbf{r}_p^\dagger = -\frac{m_e^\dagger}{M^0}\mathbf{r}^\dagger, \quad \gamma_{\rm cm}(\mathbf{r}_e - \mathbf{r}_p) = \gamma_{\rm cm}\mathbf{r}$$
$$= \mathbf{r}_e^\dagger - \mathbf{r}_p^\dagger = \mathbf{r}^\dagger = \frac{\mathbf{r}^0}{\gamma^\dagger}; \quad \gamma_{\rm cm}t = \frac{t^0}{\gamma^\dagger} = t^\dagger, \quad \frac{\mathscr{M}}{\gamma_{\rm cm}} = \mathscr{M}^\dagger = \gamma^\dagger\mathscr{M}^0, \quad \boldsymbol{\upsilon}(= \frac{d\mathbf{r}}{dt}) = \frac{d\mathbf{r}^\dagger}{dt^\dagger} = \boldsymbol{\upsilon}^\dagger. \qquad (9)$$

Accordingly $\upsilon_e = \upsilon_e^\dagger$, $\upsilon_p = \upsilon_p^\dagger$, $\mathbf{L} = \mathbf{L}^\dagger = \mathbf{r}^\dagger \times (\mathscr{M}^\dagger\upsilon^\dagger)$.

Finally, on transforming from the $\mathbf{R}_e^L, \mathbf{R}_p^L$ to $\mathbf{r}^L, \mathbf{R}^L$ coordinates described now in the Lab frame, it is taken as a basic requirement that the total energy should be invariant: $m_e^L c^{L2} + m_p^L c^{L2} = M^L c^{L2} + \mathscr{M}^L c^{L2}$. This, for $m_e^L = m_p^L$, $m_e = m_p$ and hence $\gamma_{\rm cm}^{L\prime} = \gamma_{\rm cm}^{L\prime\prime}$ (Eqs 6.3a,b), becomes $2\gamma_{\rm cm}^{L\prime} m_p c^{L2} = 2m_p c^{L2} + \gamma_{{\rm cm},r}^L m_p c^{L2}$, or $\gamma_{\rm cm}^{L\prime} = 1 + \frac{1}{2}\gamma_{{\rm cm},r}^L$.

2.3 Feasible trajectories of motions of the e, p of a highly relativistic bound stationary system We are seeking to establish a system of bound e, p at such a small separation that necessitates the e, p relative velocity υ to be very close to c (Sec 5), hence $\gamma >> 1$. From this and Eqs (7),(8), it follows that characteristically, $\gamma_e, \gamma_p, \gamma_{\rm cm} >> 1$, i.e. the e, p and their centre of mass CM must be moving at velocities very close to c^L in the Lab frame. Furthermore, the quantum condition (Sec 2.5) restricts the e, p relative orbit $l(= 1)$ to be quantised in radius (r_l) and in orientation ($\vartheta_{\mp l}$). Thirdly, in representing a single particle neutron, we require the e, p system to be stationary and that, if not acted by an external force, the CMN is at rest; or more generally the motion of the system as a whole to be that of the CMN under an external force.

Qualitatively, the simplest if not the only possible trajectories of motions of the e, p having all the above features is evident: The e, p total motions are along the outer and inner circles of radii R_e, R_p about a Z axis passing the CMN in the lower and upper planes normal to the Z axis or, parallel to the X, Y plane; the origin of the coordinates X, Y, Z coincides with the CMN here. Accordingly the CM moves along the co-centred middle circle of radius R in the X, Y plane. See Fig 1c. All with constant velocities. Kinemetically, the e, p relative motion, with their reduced mass moving along orbit l, is therefore produced because the velocities $\mathbf{u}_e, \mathbf{u}_p$ of their total motions along the circles of radii R_e, R_p are at a (fixed) finite angle, not collinear. (Dynamically, it is the presence of an interaction force which results in the non-collinear total motions of the e, p.) So, the relative orbit l as a whole must be in circular motion following the CM along the circle of radius R, in such a way that $\mathbf{r}_e, \mathbf{r}_p$ end always on the circles of radii R_e, R_p; see Fig 1c. So the e, p separation $\mathbf{r}_e - \mathbf{r}_p = \mathbf{r}_l$ as projected in the X, Y plane, $(\mathbf{r}_e - \mathbf{r}_p)_{XY}$, rotates about a z axis passing the CM and paralell with Z. As described in the X, Y, Z coordinates, in the meantime that the z axis moves along the circle of radius R following the CM, the normal of the orbit l–plane precesses about the z axis.

For a set of relative coordinates x, y, z we further specify the x, y plane to be parallel with the X, Y plane, and the x axis to be along the direction of $(\mathbf{r}_e - \mathbf{r}_p)_{X,Y}$. So the x, y axes are re-oriented about the z axis at the rate of the rotation of $(\mathbf{r}_e - \mathbf{r}_p)_{X,Y}$ continuously, but statically — no velocity and inertia are attached to the x, y axes. Instead, on a dynamically equivalent footing, the particle of mass $\mathscr{M}$ rotates along the orbit l of radius $r_l = |\mathbf{r}_e - \mathbf{r}_p|$; the axis of rotation is at a fixed angle ϑ (equal to $\vartheta_{\mp l}$ and in turn to $\vartheta_{\mp l'}$) to the z axis and lies always in the x, z plane, as in Fig 1b. That is, relative to the coordinates x, y, z, the axis of rotation of $\mathscr{M}$ along the orbit l has a fixed orientation, no precession. We now have two representations of the same angular motion.

2.4. Neutron mass Let the neutron be now in slow motion at velocity u_n^L in $+X$ direction in the Lab frame during a time Δt^L in which the neutron mass is measured. At any instant

of time the neutron thus has a total mass $m_n^{L\prime} = \gamma_n'(u_n^{L\prime})M^0$ moving at a total velocity $u_n^{L\prime} = u_n^L + u_{\mathrm{cm}X}^L$ in the X direction, where $\gamma_n' = (1-(u_n^{L\prime})^2/c^{L2})^{-1/2}$, $u_{\mathrm{cm}X}^L = u_{\mathrm{cm}}^L \sin\Phi$, $\Phi = \angle(\mathbf{R}^L, X^L)$. For u_{cm}^L, u_n^L orthogonal and ${u_n^L}^2/c^{L2} << 1$, $\gamma_n'(u_n^{L\prime}) \simeq \gamma_{\mathrm{cm}X}^L(u_{\mathrm{cm}X}^L)\gamma_n(u_n^L)$, where $\gamma_{\mathrm{cm}X}^L = (1-{u_{\mathrm{cm}X}^L}^2/c^{L2})^{-1/2}$, and $\gamma_n(u_n^L) \simeq 1$. With $u_{\mathrm{cm}}^L \simeq c^L$ (Sec 5) and the experimental magnetic radius of neutron 8.6×10^{-16} m for R^L, the M^L rotation period about the CMN is estimated $T_{\mathrm{cm}}^L = 2\pi R^L/u_{\mathrm{cm}}^L \simeq 2\times10^{-23}$ s, which is $<< \Delta t^L$ typically of nano seconds or longer. The measurement thus informs the expectation value of $m_n^{L\prime}$ during Δt^L, $m_n^L = \langle m_n^{L\prime}\rangle = \langle\gamma_n'\rangle M^0 \simeq M^0$, where $\langle\gamma_n'\rangle \simeq \gamma_{\mathrm{cm}X}^L(\langle u_{\mathrm{cm}X}^L\rangle) = 1$, $\langle u_{\mathrm{cm}X}^L\rangle = \frac{u_{\mathrm{cm}}^L}{2\pi}\int_0^{2\pi}\sin\Phi d\Phi = 0$.

2.5. Eigenvalue equations. Orbital and precessional angular momenta. Antineutrino In the absence of applied force and omitting the very weak gravity, M is hence free and not directly subject to quantisation condition. We thus need only to establish the relativistic Schrödinger or Klein-Gordon equation (KGE) for the mass $\mathscr{M}$ in the CM frame, represented here by the spherical polar coordinates r,ϑ,ϕ corresponding directly to the relative coordinates x,y,z. The KGE has the usual form $[(E_{tot_{op}}-V)^2 - {\mathscr{M}^0}^2c^4 - p_{op}^2c^2]\psi_{tot} = 0$. More relevant to the highly relativistic system here is the square-root (SQR) form of the KGE: $H_{op}\psi = H\psi$, where $H_{op} = (E_{tot_{op}}-V) - \mathscr{M}^0c^2 + V = \frac{\gamma}{(\gamma+1)}\frac{p_{op}^2}{\mathscr{M}} + V$ and $p_{op}^2 = (\mathscr{M}\upsilon_r)^2/\mathscr{M} + (L^2)_{op}/\mathscr{M}r^2$ are the Hamiltonian and squared linear momentum operators associated with the kinetic motion of $\mathscr{M}$. For the e,p interaction potential V being central (Sec 3), whence $V(\mathbf{r}) = V(r)$, the wave function of $\mathscr{M}$, $\psi(r,\vartheta,\phi)$, may be written as $\psi = \mathcal{R}(r)\mathcal{Y}(\vartheta,\phi)$. And either the KGE or SQR-KGE separates out an eigen value equation for the squared (relative orbital) angular momentum operator $(L^2)_{op}$,

$$(L^2)_{op}\mathcal{Y}(\vartheta,\phi) = L^2\mathcal{Y}(\vartheta,\phi), \quad (L^2)_{op} = -\hbar^2\left(\frac{\partial^2}{\partial\vartheta^2} + \cot\vartheta\frac{\partial}{\partial\vartheta} + \frac{1}{\sin^2\vartheta}\frac{\partial^2}{\partial\phi^2}\right). \tag{10}$$

(10) may be solved without $V(r)$ being explicitly known. The eigen functions are the spherical harmonics, $\mathcal{Y}_l^m = C_l^m P_l^m(\cos\vartheta)e^{im\phi}$. The square-root eigen values and their z components are

$$L_l = |\mathbf{r}_l\times(\mathscr{M}\boldsymbol{\upsilon}_{tl})| = \sqrt{l(l+1)}\,\hbar, \quad L_{z,m} = \mp L_l\cos\vartheta_l = m\hbar, \quad l = 0,1,\ldots; m = 0,\ldots,\mp l. \tag{11}$$

For an lth state, by the expression $\mathbf{r}_l\times(\mathscr{M}\boldsymbol{\upsilon}_{tl})$, $\mathscr{M}$ rotates along a circular orbit l about a rotation axis at angle ϑ_m to the z axis.

Owing to their having a finite (radial) acceleration, $\mathsf{a}_l = -|d^2\mathbf{r}_l/dt^2|(\mathbf{r}_l/r_l)$, as a well-known non-inertial frame effect the e,p with intrinsic spins $(\frac{1}{2})$ each in addition execute a Thomas precession—at an angular velocity $\boldsymbol{\omega}_T$ about the z axis. The precession is from the perspective of the X,Y,Z coordinates, in the same way as $\mathscr{M}$ executes orbital angular motion therein but in the opposite sense. So the orbital tangential and angular velocities, $\boldsymbol{\upsilon}_{tl} = \boldsymbol{\omega}_o\times\mathbf{r}_l$ and $\boldsymbol{\omega}_o = (\upsilon_{tl}/r_l)\hat{\vartheta}_m$, are modified to the precessional–orbital ones as $\boldsymbol{\upsilon}_l(\equiv\boldsymbol{\upsilon}_{tl'}) = \boldsymbol{\omega}\times\mathbf{r}_l$ and $\boldsymbol{\omega} = (\omega_o-\omega_T)\hat{\theta}_m$, the angle ϑ_m of the normal of the orbit l at the z axis to $\theta_m \equiv \vartheta_{m'}$, and L_l to $Ł_l \equiv L_{l'}$; $\mathbf{r}_l$ is unchanged because of quantisation. $\boldsymbol{\omega}_T = (\gamma^2/(\gamma+1))\mathsf{a}_l\times\boldsymbol{\upsilon}_l/c^2$ according to Thomas and is in the direction $-\mathbf{r}_l\times\boldsymbol{\upsilon}_l = -\mathbf{Ł}_l/\mathscr{M}$, i.e. opposite to $\mathbf{Ł}_l$.

For the e,p spin-up state, hence $m=-l$, the total e,p spin angular momentum relative to the CM in the z direction is (Eq 16, Sec 2.6) $S_z = \frac{1}{2}\hbar$. From the requirement of angular momentum conservation for the bound e,p subject to no exchange of angular momentum with the surrounding, it follows that their precessional angular momentum $\mathbf{L}_T = \mathbf{r}_l\times(\mathscr{M}\boldsymbol{\upsilon}_T)$ projected in z direction, $L_{Tz} = -L_T\cos\theta_m$, must be $L_{Tz} = S_z = \frac{1}{2}\hbar$ for $m=-l$, $\theta_m = \theta_{-l} = \pi-\theta_l$; and $L_{Tz} = S_z = -\frac{1}{2}\hbar$ for $m=l$, $\theta_m = \theta_l$. The total relative precessional–orbital angular momenta $Ł_l$ and their z components $Ł_{z,m}(\equiv L_{z,m'})$ thus follow to be

$$Ł_l = L_l - L_T = |\mathbf{r}_l\times(\mathscr{M}\boldsymbol{\upsilon}_l)| = \sqrt{l'(l'+1)}\,\hbar = \frac{\sqrt{(4l^2-1)}\,\hbar}{2}, \quad l' = l-\tfrac{1}{2} = \ldots,-\tfrac{3}{2},-\tfrac{1}{2},\tfrac{1}{2},\ldots; \tag{12a}$$

$$Ł_{z,m} = Ł_l\cos\theta_m(\equiv Ł_{l'}\cos\vartheta_{m'}) = \mp Ł_l\cos\theta_l = m'\hbar, \quad m' = \mp\tfrac{1}{2},\ldots,\mp l'. \tag{12b}$$

$$\text{For } l=1\ (l'=\tfrac{1}{2},\ m'=\mp\tfrac{1}{2}): \quad Ł_1 = |\mathbf{r}_1\times(\mathscr{M}\boldsymbol{\upsilon}_1)| = \tfrac{\sqrt{3}\,\hbar}{2}, \quad Ł_{z,\mp1} = r_1\mathscr{M}\upsilon_1\cos\theta_{\mp1} = \mp\tfrac{\hbar}{2} \tag{13}$$

The $l = 1$ ($l' = \frac{1}{2}$) states describe a ground-state neutron (Sec 3). (13a) thus gives the e, p relative precessional–orbital angular momentum internal of the neutron, and (13b) the two possible z components associated with a minimum-energy ($m = -1, m' = -\frac{1}{2}$) and excitation ($m = 1, m' = \frac{1}{2}$) state in an external (applied or random environmental) magnetic field in the $+z$ direction. By the expression $\mathbf{r}_1 \times (\mathscr{M}\boldsymbol{v}_1)$ in (13), $\mathscr{M}$ moves along a circular orbit of radius vector $\mathbf{r}_1$ about the CM in the x', y' plane, where $\angle x', x = \theta_1$, $y' = y$; see Fig 1b. For $m' = -\frac{1}{2}$, the rotation is in clockwise sense, or, the normal $\mathbf{n}$ of the rotation plane is at angle $\pi - \theta_1$ to the z axis as in Fig 1b. And conversely for $m' = \frac{1}{2}$. The vectors $\mathbf{Ł}_1$ are in the directions of the normals, i.e. at angles $\theta_{-1} = \pi - \theta_1$ and θ_1 to the z axis; $\theta_1 = \arccos(Ł_{z,1}/Ł_1) = \arccos(1/\sqrt{3}) = 54.7^o$. For the next orbital, $l = 2$ ($l' = \frac{3}{2}$), $Ł_{z,2}/Ł_2 = (3/2)/(\sqrt{15}/2) = 0.775$, $\theta_2 = 39.2^o$.

Finally, for the neutron existing (in zero applied field) only in a single non-degenerate state $l = 1$ and presuming that, in terms of the SQR-KGE here, energies of different l and same n are degenerate, then N (the radial degree of freedom)$= 0$ and $n = N + l + 1 = 0 + l + 1 = 2$. So $= T_{r,1} = 0$, and the total kinetic energy of $\mathscr{M}$ is, with $Ł_1$ for L_1, $T_1 = T_{t,1} = \frac{\gamma\mathscr{M}v_1^2}{(\gamma+1)} = \frac{\gamma L_1^2}{(\gamma+1)\mathscr{M}r_1^2} = \frac{3\gamma\hbar^2 M}{4(\gamma+1)m_e m_p r_1^2}$.

From the trajectory of motion of the reduced mass $\mathscr{M}$ of e, p above and the physical trajectories of the total motions of the e, p (Sec 2.3) combinatorially, it follows that the physical trajectories of the e, p partial-relative and relative motions are ellipses in the lower, upper and the x, y planes; the latter is the projection of the $l = 1$th circular orbit (Fig 1b). Disregarding their charges, the neutral vortex associated with the e, p relative precessional–orbital motion in the x, y plane, which carries one unit half-integer quantum of the angular momentum $Ł_{z,\mp 1} = \mp\frac{1}{2}\hbar$ and (paper II) has a positive helicity, resembles directly an antineutrino $\bar{\nu}_e$ here confined within the neutron. The spin angular momentum of $\bar{\nu}_e$ hence is

$$S_{\bar{\nu}_e} = Ł_{z,\mp 1} = \mp\tfrac{1}{2}\hbar = \mp s_{\bar{\nu}_e}\hbar, \quad s_{\bar{\nu}_e} = \tfrac{1}{2}. \tag{14}$$

2.6. Electron, proton and neutron spins Certain external, random environmental in the case of zero applied, magnetic field would always present and hence sets the (instantaneous) z axis here. The intrinsic spin angular momenta of $\alpha = e, p$ in their rest frames are $S^0_\alpha \equiv S^0 = \sqrt{s_\alpha(s_\alpha+1)}\,\hbar = \frac{\sqrt{3}}{2}\hbar$, where $s_\alpha = \frac{1}{2}$, and for spin-up states are at angles θ^0_α to the direction of the z axis; the z components are $S^0_{\alpha z} = S^0_\alpha \cos\theta^0_\alpha = \frac{1}{2}\hbar$. For the e, p separation r_1 being comparable to the sizes of the e, p charges (Secs. 3,5), we need to treat the latter explicitly as extended objects, here simply as spheres of radii a^0_e, a^0_p in the e, p rest frames. Suppose that the mass of each particle, say m^0_e of e, is predominantly located in its charge (thus negligibly in its wave field) and is distributed throughout the charge sphere with a density $\rho_{m_e}(\boldsymbol{\xi}^0_e)$; and its charge $-e$ along the circular loop at the intersection of the surface of the charge sphere with the plane normal to the spin axis and containing $\mathbf{R}_e$. So S^0_e is given rise to by the angular motion of the sphere at angular and tangential velocities $\omega^0_e = d\phi^0_e/dt^0_e$ and $v^{s0}_e = a^0_e\omega^0_e$ about the spin axis $\mathbf{n_e}$ passing $\mathbf{R}_e$, with mass element $d\mathbf{m}^0_e = m^0_e\rho_{m_e}(\boldsymbol{\xi}^0_e)d^3\boldsymbol{\xi}^0_e$,

$$S^0_e = m^0_e \textstyle\int |\boldsymbol{\xi}^0_e \times \boldsymbol{v}^{s0}_e|\rho_{m_e}(\boldsymbol{\xi}^0_e)d^3\boldsymbol{\xi}^0_e = \frac{1}{g_e}a^{0\,2}_e\omega^0_e m^0_e = \frac{\sqrt{3}}{2}\,\hbar\ ; \quad S^0_{ez} = \frac{1}{g_e}a^{0\,2}_e m^0_e\omega^0_e\cos\theta^0_e = \frac{1}{2}\hbar \tag{15}$$

where g_e is the Lande g factor.

In the CM frame, the radius of the e charge sphere weighed with respect to the CM at $\mathbf{R}$ is $a_e = \frac{m_p}{M}a$, where a is related with a_e in analogy to r with r_e (Eq 2g); and $a = \frac{a^0}{\gamma_a}$, where γ_a is an effective Lorentz factor (see Appendix A). The distance of a point on the charge sphere of e to the CMN is $\mathbf{R}^s_e$, and to the CM is $\mathbf{r}^s_e = (\mathbf{R}^s_e - \mathbf{R}) = \frac{m_p}{M}\mathbf{r} + \boldsymbol{a}_e = \frac{m_p}{M}(\mathbf{r} + \boldsymbol{a})$. To an observer rotating with $\boldsymbol{a}_e$ or $\boldsymbol{a}$ about the spin axis, $\mathbf{r}$ changes direction continuously over a 2π angle in the rotation plane. So the magnitudes of the time-averages of $\mathbf{r}^s_e$ and its first derivative in the rotation plane are $|\langle\mathbf{r}^s_e\rangle| = a_e = \frac{m_p}{M}a$, $|\langle\boldsymbol{v}^s_e\rangle| = |\frac{d\langle\mathbf{r}^s_e\rangle}{dt}| = a_e\omega_e = \frac{m_p}{M}a\omega_e$, where $\omega_e = \frac{d\phi_e}{dt} = \frac{d\phi_e}{d(t^0/\gamma)}$. And similarly for p. The z components of the partial spins, $S_{e,\mathrm{cm}z}$, $S_{p,\mathrm{cm}z}$ and of the total spin,

S_z, of e, p described with respect to the CM are thus formally

$$S_{e,\mathrm{cm}z} = \tfrac{1}{g_e}\langle \mathbf{r}_e^s\rangle^2\omega_e m_e\cos\theta_e = \tfrac{1}{g_e}a_e(\tfrac{m_p}{M}a)\omega_e m_e\cos\theta_e = \tfrac{m_p}{M}S_{ez},\quad S_{ez} = \tfrac{1}{g_e}a_e a\omega_e m_e\cos\theta_e$$
$$= S^0_{ez} = \tfrac{1}{2}\hbar;\quad S_{p,\mathrm{cm}z} = \tfrac{m_e}{M}S_{pz},\qquad S_{pz} = \tfrac{1}{g_p}aa_p\omega_p m_p\cos\theta_p = S^0_{pz} = \tfrac{1}{2}\hbar;$$
$$S_z = S_{e,\mathrm{cm}z} + S_{p,\mathrm{cm}z} = \tfrac{m_e S^0_{ez} + m_p S^0_{pz}}{M} = S^0_z = \tfrac{1}{2}\hbar \tag{16}$$

Spin invariance has been imposed in going from the rest to the CM frame. The detailed transformation relations for θ_e (which would approach zero if $\gamma_e >> 1$), ϕ_e and θ^0_e, ϕ^0_e, are not evoked here. The spin (dipole) magnetic moment, μ^{s0}_e of e in the rest frame for example, is accordingly produced by the current loop of charge $-e$, area $\pi {a^0_e}^2$, and angular velocity ω^0_e in the $\pi - \theta^0_e$ direction. Its z components corresponding to the $S_{e,\mathrm{cm}z}, S_{ez}$ in the CM frame are

$$\mu^s_{e,\mathrm{cm}z} = e\frac{\omega_e}{2\pi}\pi\langle r^s_e\rangle^2\cos(\pi-\theta_e) = -\frac{g_e e(m_p/M)S_{ez}}{2m_e} = \frac{m_p}{M}\mu_{ez},\quad \mu^s_{ez} = -\frac{g_e eS_{ez}}{2m_e} = -\frac{g_e e\hbar}{4m_e}. \tag{17}$$

For the e, p to be in a bound, minimum magnetic energy state (Sec 3), apart from $l(= l' + \frac{1}{2}) = 1$, $m(= \mp(m' + \frac{1}{2})) = \mp 1$ (Sec 2.5), S_{ez}, S_{pz} need be parallel mutually and each antiparallel to $Ł_{z,m}$ (Figs 1a,b). $Ł_{z,m}, S_{ez}, S_{pz}$ can therefore assume two possible configurations

$$(i)\ \ Ł_{z,\text{-}1} = -\tfrac{1}{2}\hbar,\ \ S_{ez} = \tfrac{1}{2}\hbar,\ \ S_{pz} = \tfrac{1}{2}\hbar;\quad (ii)\ \ Ł_{z,1} = \tfrac{1}{2}\hbar,\ \ S_{ez} = -\tfrac{1}{2}\hbar,\ \ S_{pz} = -\tfrac{1}{2}\hbar. \tag{18}$$

The total angular momentum J_l and the z components $J_{z,m}$ of J_l of the $l(= l' + \frac{1}{2}) = 1$ state, whence the neutron spin angular momentum $\mathbf{S}_n \equiv -\mathbf{J}_1$ and z components $S_{nz} \equiv -J_{z,\mp 1}$, where the negative signs are by assignment, based on the vector addition model are

$$S_n = J_{l=1} = \sqrt{j(j+1)}\hbar|_{l=1} = \sqrt{s_n(s_n+1)} = (\sqrt{3}/2)\hbar, \tag{19}$$

where $s_n = j|_{l=1} = [(s_e + s_p) - l']_{l=1} = (\frac{1}{2} + \frac{1}{2}) - \frac{1}{2} = \frac{1}{2}$, and for the spin- down and up states

$$S_{nz} = -J_{z,m}|_{m=\text{-}1} = -[(S_{pz+} + S_{ez+}) + Ł_{z,\text{-}1}] = -[(\tfrac{1}{2} + \tfrac{1}{2}) - (1 - \tfrac{1}{2})]\hbar = -s_n\hbar = -\tfrac{1}{2}\hbar,$$
$$S_{nz} = -J_{z,m}|_{m=1} = -[(S_{pz\text{-}} + S_{ez\text{-}}) + Ł_{z,1}] = -[(-\tfrac{1}{2} - \tfrac{1}{2}) + (1 - \tfrac{1}{2})]\hbar = s_n\hbar = \tfrac{1}{2}\hbar. \tag{20}$$

As the $\mathbf{Ł}_1$, $\mathbf{S}_n$ may be at angle $\theta_{\text{-}1} = \pi - \theta_1$ (for $m = -1$) or θ_1 (for $m = 1$) to the z axis. By assigning to it the negatives of $J_{z,\mp 1}$ in (20), S_{nz} has the same sign as $Ł_{z,\mp 1} = \mp\frac{1}{2}\hbar$, which by virtue of its physical role may be identified to be responsible for the (apparent) neutron magnetic moment (μ_{nz}) as manifested in resonance experiment. The corresponding instantaneous z component of magnetic moment is, e.g. for $m_l = -1$, $\mu_{z,\text{-}1} = -eŁ_{z,\text{-}1}/(2\mathscr{M}) = e\hbar/(4\mathscr{M})$. For the case $m_e = m_p$, $\mathscr{M} = \frac{m_p}{2} = \frac{\gamma_p m^0_p}{2} = \frac{\gamma_{\mathrm{cm}} m^0_p}{4}$ (see after Eqs 8). So $\mu_{z,\text{-}1} = \frac{4e\hbar}{4\gamma_{\mathrm{cm}} m^0_p}$, and $\mu_{nz} = \langle\mu_{z,\text{-}1}\rangle = \frac{4e\hbar}{4\langle\gamma_{\mathrm{cm}}\rangle m^0_p} = \frac{1}{2}g_n\mu_N$, where $g_n = 4$ gives the neutron g factor, which agrees approximately with the experimental value $g^{exp}_n = 3.826$; $\mu_N = \frac{e\hbar}{2m^0_p}$ (the nuclear magneton).

3. Electron–proton electromagnetic interaction

We shall below derive for the electron e and proton p comprising the model neutron their interaction force $\mathbf{F}$, the corresponding potential V and stationary-state Hamiltonian H based on first principles laws of electromagnetism and (the solutions of Sec 2 of) relativistic quantum-mechanics. We shall continue to work in the CM frame and using the variables with respect to M, which will directly enter the electromagnetic interactions below, and for simplicity the time t instead of t_e, t_p; the local time t_e, t_p effect will be included afterward by a projecting factor. In the current Sec 3, the vector $\mathbf{r}$ or $\mathbf{r}_l$ refers to the e, p separation distance which begins at $\mathbf{R}_p$ and ends at $\mathbf{R}_e$ (Figs 1a, c); its magnitude is equal to that of $\mathbf{r}$ or $\mathbf{r}_l$ of Sec 2.5, Fig 1b.

Consider the e,p system in the $l(=l'+\frac{1}{2})$, $m=-l(=-(l'+\frac{1}{2}))$ state (Fig 1a); S_{pz}, S_{ez} are assumed in the $+z$ direction, i.e. antiparallel with $L_{z,\text{-}1}$ (Figs 1a,b). Firstly the proton of a charge $+e$ produces at the electron at $r=r_l$ apart a (transformed) Coulomb field $\mathbf{E}_p(r_l)=(e/4\pi\epsilon_0 r_l^2)\,\hat{\mathbf{r}}$ (in SI units here and below); $\hat{r}$ is an unit vector pointing from p to e. E_p is amplified from its rest-frame value E_p^0 by a factor $\propto(1/r^2)/(1/(r^0)^2)=\gamma^2=1/f_c$ and hence has a narrowed profile at a point $\mathbf{r}$ perpendicular to its motion ϕ direction by an inverse factor, f_c; and so are the magnetic fields below. Furthermore, the proton is in relative precessional–orbital and spin motions at the velocities $\boldsymbol{v}_p$ and, on average in the plane normal to the z axis, $\langle\boldsymbol{v}_p^s\rangle\cos\theta_p$, which projected in the $x'y'$ plane is $\langle\boldsymbol{v}_p^s\rangle''=\langle\boldsymbol{v}_p^s\rangle\cos\theta_p\cos\theta_l$. So p produces at e magnetic fields $\mathbf{B}_p^{orb}(=-\boldsymbol{v}_p\times\mathbf{E}_p)$ and $\mathbf{B}_p^s(=-\langle\boldsymbol{v}_p^s\rangle''\times\mathbf{E}_p)$ along the θ_l direction given as (the transformed Biot-Savart law),

$$\mathbf{B}_p^{orb}=\frac{e\boldsymbol{v}_p\times\mathbf{r}_l}{4\pi\epsilon_0c^2r_l^3}=-\frac{e\mathbf{r}_l\times(\frac{m_em_p}{M})\boldsymbol{v}_l}{4\pi\epsilon_0m_pc^2r_l^3}=-\frac{\sqrt{4l^2-1}\;e\hbar\;\hat{\theta}_l}{8\pi\epsilon_0m_pc^2r_l^3};\quad \mathbf{B}_p^s(r\mp\bar{a})=\frac{\mp\frac{1}{2}e\langle\bar{\boldsymbol{v}}_p^s\rangle''\times(\mathbf{r}_l/r_l)}{4\pi\epsilon_0c^2(r\mp\bar{a})^2},$$

$$\mathbf{B}_p^s(r_l)=\mathbf{B}_p^s(r_l-\bar{a})+\mathbf{B}_p^s(r_l+\bar{a})=\frac{-e\bar{a}\langle\bar{\boldsymbol{v}}_p^s\rangle''\times(\mathbf{r}_l/r_l)}{2\pi\epsilon_0c^2r_l^3(1-\frac{\bar{a}^2}{r_l^2})^2}=\frac{-\eta^2g_pe\hbar\cos\theta_l\hat{\theta}_l}{4\pi\epsilon_0m_pc^2r_l^3C_{1l}},\quad C_{1l}=\left(1-\tfrac{\bar{a}^2}{r_l^2}\right)^2 \tag{21}$$

In Eq (21a) we used (4b) for $\boldsymbol{v}_p$ and (12a) for $\mathbf{r}_l\times(\frac{m_em_p}{M})\boldsymbol{v}_l$. For writing Eq (21b), we represented the spin current loop (Sec 2.6) effectively as two-half charges $+\frac{e}{2},+\frac{e}{2}$ located at $-\bar{a},\bar{a}$ from $\mathbf{R}_p$ on the x' axis and moving oppositely at velocities $-\langle\bar{v}_p^s\rangle'',\langle\bar{v}_p^s\rangle''$ in the $-y,+y$ directions, where $\bar{a}=\eta a$, $\langle\bar{v}_p^s\rangle''=\eta\langle v_p^s\rangle''$. $\eta=1/\sqrt{2}$ so that the moment of inertia with respect to e is equivalent to the original one. In Eq (21c) we used $\bar{a}\langle\bar{v}_p^s\rangle m_p\cos\theta_p/g_p=\eta^2S_{pz}=\eta^2\frac{\hbar}{2}$ given after (16d).

In the $\mathbf{E}_p$, $\mathbf{B}_p^{orb}+\mathbf{B}_p^s=\mathbf{B}_p$ fields of the proton (cf Fig 1a), the electron at $|\mathbf{r}|=r_l$ apart, with an effective charge $q_e=-f_ce$, and in precessional–orbital and spin motions at the velocity $\boldsymbol{v}_e$ and $\langle\boldsymbol{v}_e^s\rangle$, is acted by an electromagnetic force along the $\mathbf{r}$ direction according to the Lorentz force law,

$$\mathbf{F}_{pe}(r_l)[\equiv\mathbf{F}_{pe}(r_l,t_e,t_p)]=-f_ce\mathbf{E}_p(r_l)+f_t[\mathbf{F}_{pe,m}^{orb-orb}(r_l,t)+\mathbf{F}_{pe,m}^{s-orb}(r_l,t)+\mathbf{F}_{pe,m}^{s-s}(r_l,t)], \tag{22}$$

$$\text{where}\quad \mathbf{F}_{pe,m}^{orb-orb}=-e\boldsymbol{v}_e\times\mathbf{B}_p^{orb}=-\frac{e\mathbf{r}_l\times(\frac{m_em_p}{M}\boldsymbol{v}_l)}{m_er_l}B_p^{orb}=-\frac{(4l^2-1)e^2\hbar^2\;\hat{r}}{16\pi\epsilon_0m_em_pc^2r_l^4}, \tag{23}$$

$$\mathbf{F}_{pe,m}^{s-orb}=-e\boldsymbol{v}_e\times\mathbf{B}_p^s=-\frac{e\mathbf{r}_l\times(\frac{m_em_p}{M}\boldsymbol{v}_l)}{m_er_l}|\mathbf{B}_p^s|=\frac{(2l-1)\eta^2g_pe^2\hbar^2\;\hat{r}}{8\pi\epsilon_0m_em_pc^2r_l^4C_{1l}}, \tag{24}$$

$$\mathbf{F}_{pe,m}^{s-s}=-\frac{\partial V_{pe,m}^{s-s}}{\partial r_l}\;\hat{r}=|\boldsymbol{\mu}_{ez}^s\cos\theta_l|\frac{\partial|\mathbf{B}_p^s|}{\partial r_l}\;\hat{r}=-\frac{3\eta^2g_eg_pe^2\hbar^2\cos^2\theta_l\;\hat{r}}{16\pi\epsilon_0m_em_pc^2r_l^4C_{1l}}. \tag{25}$$

f_c is the fraction of the e-charge sphere momentarily facing the narrowed $\mathbf{E}_p$ profile at $\mathbf{r}_l$. Eq (4a) for $\boldsymbol{v}_e$ and again (12a) for $r_l(\frac{m_em_p}{M})\upsilon_l$ are used in (23),(24). In (25), $V_{pe,m}^{s-s}=-|\boldsymbol{\mu}_{ez}^s||\mathbf{B}_p^s|\cos\theta_l$ is the magnetic potential of the spin-spin interaction; $\boldsymbol{\mu}_{ez}^s$ is an intensive quantity at $\mathbf{r}$, hence not affected by the B_p profile narrowing, and is given by Eq (17b). $\mathbf{F}_{m0}^{s-s}=-\int_0^{2\pi}e\boldsymbol{v}_e^s\times\mathbf{B}_{pz}^s(r_l)d\phi_e^s=0$; $\frac{\partial|\mathbf{B}_{pz}^s|}{\partial r_l}=-\frac{3B_{pz}^s}{r_l}$; f_t projects the product of υ_e,υ_p contained in each component magnetic force to that of υ_e',υ_p' which actually enter the e,p interaction. $\upsilon_e'\upsilon_p'=(M/m_p)\upsilon_e(M/m_e)\upsilon_p=f_t\upsilon_e\upsilon_p$ (Sec 2.1), so $f_t=M/\mathscr{M}$. A short ranged repulsion $\mathbf{F}_{pe}^{rep}=A_{rep}\hat{r}/r_l^{N+1}$ may generally also present but is omitted for the intermediate range of interest here. Given the $S_{ez},S_{pz},L_{z,\text{-}1}=\frac{1}{2},\frac{1}{2},-\frac{1}{2}$ configuration, all the three component magnetic forces (for $l>0$ for $F_{pe,m}^{orb-orb},F_{pe,m}^{s-orb}$) acted by p on e above are in the $-\mathbf{r}$ direction and hence attractive. $\mathbf{F}_{pe}$ is therefore in the $-\mathbf{r}$ direction and maximally attractive.

Similarly, e produces at p at r_l apart the fields $\mathbf{E}_e(r_l)$ and $\mathbf{B}_e(r_l)$, and electromagnetic forces given as $f_ce\mathbf{E}_e$, $f_t\mathbf{F}_{ep,m}^{orb-orb}=-f_t\mathbf{F}_{pe,m}^{orb-orb}$, $f_t\mathbf{F}_{ep,m}^{s-orb}=-f_t\mathbf{F}_{pe,m}^{s-orb}\frac{g_e}{g_p}$, $f_t\mathbf{F}_{ep,m}^{s-s}=-f_t\mathbf{F}_{pe,m}^{s-s}$. The action and reaction forces for the e,p in equilibrium must be equal in amplitude and opposite

in direction (Newton's third law), and may be here each represented by the geometric mean as $F=\sqrt{|\mathbf{F}_{pe}||\mathbf{F}_{ep}|}=\sum_{\lambda,\lambda'}\sqrt{|\mathbf{F}^{\lambda}_{pe}||\mathbf{F}^{\lambda'}_{ep}|}\delta_{\lambda\lambda'}$, where λ,λ' indicate the different component forces. The last equation needs to hold for the action and reaction to maintain detailed balance for any small variation of the independent variables such as $\mathbf{r}_l$. The final total (attractive) force of p on e in equilibrium in the $l, m_l=-l$ state is therefore, suffixing l after $\mathbf{F}$ explicitly, $\mathbf{F}_l(r_l)=-[f_c e\sqrt{|\mathbf{E}_p||\mathbf{E}_e|}+f_t\sum_\lambda\sqrt{|\mathbf{F}^{\lambda}_{pe,m}||\mathbf{F}^{\lambda}_{ep,m}|}]\hat{r}=-f_c e\mathbf{E}_p+f_t[\mathbf{F}^{orb-orb}_{pe,m}+\mathbf{F}^{s-orb}_{pe,m}\frac{\sqrt{g_e g_e}}{g_p}+\mathbf{F}^{s-s}_{pe,m}]$. Substituting Eqs (23)–(25) into the foregoing we obtain $\mathbf{F}_l$ in explicit and scalar form,

$$F_l(r_l)=-\frac{e^2}{4\pi\epsilon_0 r_l^2}(f_c+f_m)\simeq-\frac{e^2 f_m}{4\pi\epsilon_0 r_l^2}=-\frac{f_t e^2\hbar^2 \mathcal{C}_{0l}}{16\pi\epsilon_0 m_e m_p c^2 r_l^4}, \tag{26}$$

$$f_m=\frac{f_t\hbar^2\mathcal{C}_{0l}}{4m_e m_p c^2 r_l^2},\quad \mathcal{C}_{0l}=(4l^2-1)+\frac{(2l-1)\sqrt{g_e g_p}}{2C_{1l}}+\frac{3g_e g_p\eta^2\cos^2\theta_l}{C_{1l}}. \tag{27}$$

The negative sign indicates F_l is attractive. The approximation in Eqs (26) is given for $f_m >> f_c=1/\gamma^2$. For $l=1$, using the solution values from Sec 5 gives $f_m=\hbar^2\mathcal{C}_{01}/m_e m_p c^2 r_{1m}^2=28.2$ which is $>> f_c=1/\gamma^2=5.6\times10^{-11}$.

$l=0$ yields $L_0=0$, $B_p^{orb}=0$, and hence zero orbit-orbit and orbit-spin interactions. For $l\geq1$, the three component magnetic forces are attractive each. $l=1$ therefore is the lowest possible state of the e,p bound by a magnetic force at a separation $\sim10^{-18}$ m (Sec 5) and is the only state with the correct spin $\frac{1}{2}$ (Sec 2.6). (By a more basic consideration, higher l would lead to much shorter and hence unrealistic interaction distances for the a_e^0, a_p^0 values prescribed by nature.) The $l=1$ state is therefore an only liable candidate for the neutron. For $l=1$, hence $\cos\theta_1=1/\sqrt{3}$, and setting $m_e=m_p$ (see Sec 2.6), hence $f_t=4$, Eq (26), the corresponding interaction potential V_1 and Hamiltonian H_1 are written as, with Eqs (61f,g) for m_e, m_p, and T_1 given in Sec 2.5,

$$F_1(r_1)=-\frac{3A_o\mathcal{C}_{01}}{\gamma_e\gamma_p r_1^4},\quad A_o=\frac{e^2\hbar^2}{12\pi\epsilon_0 m_e^0 m_p^0 c^2},\quad \mathcal{C}_{01}=3+\frac{\sqrt{g_e g_p}}{2C_{11}}+\frac{\eta^2 g_e g_p}{C_{11}}; \tag{28}$$

$$V_1(r_1)=-\int_\infty^{r_1}F_1(r)dr=\frac{r_1F_1(r_1)}{3}=-\frac{A_o\mathcal{C}_{01}}{\gamma_e\gamma_p r_1^3}=-\frac{e^2\hbar^2\mathcal{C}_{01}}{12\pi\epsilon_0 m_e m_p c^2 r_1^3}; \tag{29}$$

$$T_1=C_{k1}V_1,\quad C_{k1}=\frac{9\gamma\pi\epsilon_0 Mc^2 r_1}{(\gamma+1)e^2\mathcal{C}_{01}};\quad H_1(r_1)=T_1+V_1=V_1(1-C_{k1}). \tag{30}$$

4. Neutron disintegration, β decay

Suppose that an afore-described (free) neutron, being in stationary state of a Hamiltonian H_1 at initial time, is now perturbed by an excitation or external-interaction Hamiltonian $H_I=H_I^0+H_I^1=H_I^1$ given in the CM frame; evidently $H_I^0=0$. So the bound e,p and the confined $\bar{\nu}_e$ are in the final (f) state disintegrated into free particles $e,p,\bar{\nu}_e$, with the e,p at an effective infinite separation r_∞ such that $V_1(r_\infty)=0$, whence a β decay. The reaction equation straightforwardly is $n\rightarrow p+e+\bar{\nu}_e$. The final-state total Hamiltonian has the general form $H_{1f}=V_1(r_\infty)+T_{1f}=0+T_{1f}$. On transition to the final state, provided no exchange with the surrounding, the fore-aft total angular momentum must be conserved. So the same initial-state L_1, and thus T_1, are in the final state carried by the same (though now free) $\bar{\nu}_e$. Omitting a translational kinetic energy of the emitted particles, T_{tr} as converted form the total mass difference before and after neutron decay and is experimentally known to be of MeV scale that is $<< T_1$ of GeV scale, so $T_{1f}=T_{1f}+T_{tr}\simeq T_1$, and $H_{1f}=0+T_{1f}\simeq T_1$. The energy condition for the neutron β decay to occur is $H_I=H_{1f}-H_1$. Substituting in it the equation for H_{1f} above and (30c) for H_1 gives

$$H_I=T_1-(V_1+T_1)=-V_1=\frac{A_o\mathcal{C}_{01}}{\gamma_e\gamma_p r_1^3},\quad \text{or}\quad G_F=H_I\left(\frac{4}{3}\pi r_1^3\right)=\frac{A_o C_{01}}{\gamma_e\gamma_p},\quad C_{01}=\frac{4\pi\mathcal{C}_{01}}{3}, \tag{31}$$

where $\left(\frac{4}{3}\pi r_1^3\right)$ is the volume in which the electron is confined about the proton. By virtue of its physical significance, the product term $G_{_F} = H_I(\frac{4}{3}\pi r_1^3)$ in (31b) is directly identifiable with the CM-frame counterpart of the Fermi (coupling) constant G_F^L. $G_F^L, \propto 1/\sqrt{\tau^L}$, is experimentally determined (as G_F^{exp}) from the neutron lifetime τ^L. τ^L is usually measured in the Lab frame and in a fixed direction for each neutron decay event (with a probability $\propto 1/\tau^L$) over a time interval $>> 2\pi R/u_{\rm cm}$, during which $\mathbf{u}_{\rm cm}$ explores all directions, so $\tau^L = \langle \tau/\gamma_{\rm cm}^L \rangle = \tau$ (cf also Sec 2.4). So at any instant of time t^L, $G_F^L(t^L)/G_{_F} = \sqrt{\tau}/\sqrt{\tau^L} = \sqrt{\gamma_{\rm cm}}$, whilst a measurement made during a macroscopic time informs $G_F^L = \langle G_F^L(t^L)\rangle = G_{_F}$. We shall continue to speak of $G_{_F}$.

In the GWS theory, $G_{_F}$ is given the formula $G_F^{\rm GWS} = \frac{g_{\rm w}^2\sqrt{2}(\hbar c)^2}{M_{\rm w}^2 c^4}$, where $g_{\rm w}^2 = \frac{e^2}{8\epsilon_0 \sin^2\theta_{\rm w}}$. Equating $G_F^{\rm GWS}$ with $G_{_F}$ of (31b) gives a first-principles microscopic expression for $M_{\rm w}$,

$$M_{\rm w} = \left(\frac{3\sqrt{2}\ \pi m_e m_p}{2C_{01}\sin^2\theta_{\rm w}}\right)^{1/2} = \left(\frac{3\sqrt{2}\ \pi}{2C_{01}\sin^2\theta_{\rm w}}\right)^{1/2} m_p; \quad \text{accordingly} \quad M_z = M_{\rm w}/\cos\theta_{\rm w} \tag{32}$$

In terms of the e,p-neutron model, $M_{\rm w}$ represents a specific vector mass of the e,p moving in the binding (resistive) potential field V_1, and V_1 resembles the Higgs field.

5. Numerical evaluation

Equations (28)–(31) are specified effectively by four independent variables $\bar{a}$, r_1, υ_1, and $\gamma(\upsilon_1, c)\gamma_{\rm cm}(=\gamma_e\gamma_p)$ or γ ($\gamma_{\rm cm}$ is given if γ is given), to be determined each. We need four independent constraints for quantitatively solving the dynamical variables of a realistic model neutron. It may be checked that at a r_1 value satisfying the stable-state equation (1d), the lifetime of the e,p system is not an optimum. This implies that the neutron candidate e,p system, if opted for a maximum lifetime, is not in stable state, which is on equal footing with the fact that a real free neutron indeed is "meta" stable only, with a relatively short lifetime 12 m.

Alternatively, we seek (i) the quantisation condition (13a) for $\mathcal{L}_1$‡, (ii) the experimental value of the Fermi constant, G_F^{exp}, and (iii) a maximum neutron lifetime, hence a minimum $G_{_F}$, as three basic constraints. These are (re-)written as, after dividing (13a) by $r_1\mathscr{M}^{\rm o}\upsilon_1$ for (i), and imposing the constraint (ii) on (iii),

$$(i): \qquad \gamma = \gamma_{\rm cm}\gamma^\dagger = \frac{\sqrt{3}(\hbar c)c}{2\mathscr{M}^{\rm o}c^2 r_1\upsilon_1} = \frac{D_o c}{r_1\upsilon_1}, \quad D_o = \frac{\sqrt{3}\hbar c}{2\mathscr{M}^{\rm o}c^2} \tag{33}$$

$$(ii): \qquad G_F^{exp} = 1.435853\times 10^{-62}\ \text{Jm}^3 \quad (\text{data from [1e]}) \tag{34}$$

$$(iii): \qquad G_{_F}(r_{1m}) = G_{F.min} = G_F^{exp} \tag{35}$$

Since (33) suggests that $\gamma >> 1$ for any υ_1 not too far below c, and $c = c^L$ by the standard assumption, so $\upsilon_1 = c\sqrt{\gamma^2-1}/\gamma \simeq c = c^L$, serving the fourth constraint. With this υ_1 value in (33a), and with (7b) for $\gamma_e\gamma_p(=\gamma_{\rm cm}\gamma = \gamma_{\rm cm}^2\gamma^\dagger)$ and the resultant γ from (36a) below in (31b), we obtain, for the case $\gamma^\dagger = \gamma^\dagger_{\rm max} = 459.536$,

$$\gamma = \frac{D_o}{r_1}, \quad \gamma_{\rm cm} = \frac{\gamma}{\gamma^\dagger_{\rm max}} = \frac{D_o}{\gamma^\dagger_{\rm max} r_1}, \quad G_{_F} = \frac{A_o C_{01}}{\gamma_{\rm cm}^2\gamma^\dagger_{\rm max}} = \frac{\gamma^\dagger_{\rm max}A_o C_{01} r_1^2}{D_o^2} = \frac{459.536 A_o C_{01} r_1^2}{D_o^2}. \tag{36}$$

D_o and A_o are constants. For evaluating C_{01} (Eqs 31c, 28c), we shall use $g_e = 2$, $g_p = 5.5857$; and $\eta = 1/\sqrt{2}$ (see after Eq 21). $G_{_F}$ of (36c) is then solely dependent on r_1,$\bar{a}$. Characteristically, for a specified $\bar{a}$ value, the $G_{_F}(r_1)$ vs r_1 function presents an extremal point at an (uniquely specified) r_{1m}, at which $G_{_F}(r_{1m})$ is a minimum (as in Fig 2a) but is in general not equal to G_F^{exp}. $G_{_F}(r_{1m})$

‡ The eigen solution (13a) for $\mathcal{L}_1$ directly corresponds to a Heisenberg relation for $\mathcal{L}_1$ and the angular interval 2π, or $2T_1 = C_{k1}H_1/(C_{k1}-1)$ and Δt_1. The excitation Hamiltonian H_1 is not conjugated with the Δt_1, but possibly with some other time interval Δt subjecting to a Heisenberg relation depending on the excitation scheme.

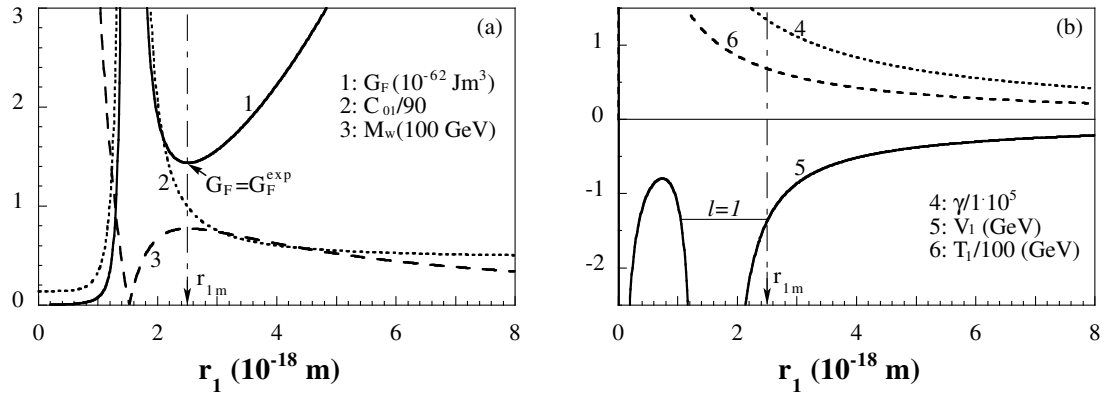

Figure 2. (a) $G_F = H_I r_1^3$, C_{01}, $M_{\rm w}$ (curves 1,2,3), and (b) γ, $V_1 = -H_I$, T_1 (curves 4,5,6) as functions of r_1 computed from Eqs (36c), (28c), (32), (36a), (29), (30a) for $\bar{a} = 1.5247 \times 10^{-18}$ m. At $r_1 = r_{1m} = 2.513 \times 10^{-18}$ m, $G_F = G_F^{exp} = 1.435853 \times 10^{-62}$ Jm^3.

increases monotonically with $\bar{a}$. Computing $G_F(r_{1m})$ as a function of $\bar{a}$ over a range of $\bar{a}$ values, a unique $\bar{a}$ is found at§ $\bar{a} = 1.5247 \times 10^{-18}$ m at which $G_F(r_{1m}) = G_F^{exp}$, $r_{1m} = 2.5130 \times 10^{-18}$ m, $\gamma = 1.3316 \times 10^5$ (Eq 36a), and $C_{01} = 88.70$ (Eqs 31c, 28c). With the $\bar{a}, r_{1m}$, (hence C_{01}), v_1, γ values obtained, all the remaining dynamical variables and functions may be evaluated.

For the fixed $\bar{a} = 1.5247 \times 10^{-18}$ m value, the computed G_F, C_{01}, $M_{\rm w}$ (where the average experimental value $\sin^2\theta_{\rm w} = 0.23$ is used), γ, $V_1(= -H_{\rm I})$, and T_1 vs. r_1 functions (Eqs 31,28a, 32, 33a, 29, 30a) are as shown in Figs 2a,b (curves 1–6). $r_1 = r_{1.\rm min}$ lies as expected in the region where $-\frac{\partial V_1(r)}{\partial r} = F_1(r) < 0$, and $V_1(r) < 0$. At $r_1 = r_{1m}$, $V_1 = -H_I = -1.35$ GeV, $T_1(\simeq \mathscr{M}c^2) = 68.0$ GeV, $H_1(\simeq E_{tot,1}) = 66.65$ GeV (Eq 30c), $M_{\rm w} = 77.23$ GeV. Furthermore specifically, with the γ value in (36b),(8a),(b), we obtain $\gamma_{\rm cm} = 289.8$, $\gamma_e = \gamma_{\rm cm}\frac{M^0}{2m_e^0} = 2.661 \times 10^5$, and $\gamma_p = \gamma_{\rm cm}\frac{M^0}{2m_p^0} \simeq \frac{\gamma_{\rm cm}}{2} = 145$, which are $>> 1$ each. So the particles e, p and their total mass M, as $\mathscr{M}$, each travel at velocities $\simeq c$ in the CM frame. The total kinetic energy of e, p in the CM frame is $T_e + T_p = 2 \times \gamma m_p c^2/(\gamma + 1) \simeq 2 \times m_p c^2 = 2 \times 136.0$ GeV which apparently is mainly consumed to contract the size of the system.

The author expresses thanks to colloquium chairman Professor J Van der Jeugt, the committee and chairman Professor J P Gazeau for providing the opportunity for presenting the research at the 30th Int Colloq on Group Theo. Meth in Phys, Ghent Univ, Belgium, and for a grant covering the author's travel expense to the colloquium, to emeritus scientist P-I Johansson for his private financial and moral support of the author's research, and to Kissemiss Johansson for his joyful companion when the unification researches were carried out. The author enjoyed very much the enlightening discussions with a number of scientists at the colloquium.

Appendix A. A formal expression for γ_a

The Lorentz transformation (5d) leads directly to the (Lorentz-Fitzgerald) contraction of the circumference $2\pi r_1$ of the $l = 1$ orbit of radius r_1, by the factor $1/\gamma$ along the direction $\boldsymbol{v}_1$. This is associated with a contraction of the de Broglie wavelength ($\lambda_d = \lambda_d^0/\gamma$) along the direction $\boldsymbol{v}_1$, which may be attributed to a source-motion resultant Doppler effect according to the IED

§ The $\bar{a}$ value is in accordance with the order of magnitude of the measured neutron charge radius, $\sim 1.4 \times 10^{-18}$ m, from electron-neutron scattering experiment. The structure of the *e-p* neutron model is in fact also supported by the neutron structure implied by the experimental scattering length, which is negative and hence suggests an attractive scattering potential as seen by a scattering electron. An attractive scattering potential for an incident electron would be precisely as expected in terms of the *e-p* neutron model, since the incident electron will be principally scattered by the intrinsically much heavier proton of the neutron. The electron of the neutron has an equally large relativistic mass but only because it rotates much faster and hence is much more distributed at any instant of time.

model. As the induced result only for the bound particles e, p here, the radius or e, p separation r_1 is also contracted by $1/\gamma$ (Eq 6.1d) in the direction transverse to $\boldsymbol{v}_1$, which has a one to one correspondence with a larger e, p attraction (Sec 3). The latter is a secondary manifestation at the same expense of the particles' high velocities compared to c as the former. A repulsion must have been counterbalanced, for otherwise the particles would have approached at closer distance without the need of higher velocities. The origin of the repulsion may be looked at in terms of electromagnetism. Given two charged particles e, p brought from infinity to a finite separation r_1, the electrostatic E field lines of their charges, and at closer distance their charges as extended entities, must now compete to occupy the same space; these are dynamical energy entities (irrespective of the signs of the charges) and must inevitably repel mutually. This is apart from the direct e-p Coulomb attraction here. (We would recognise the same origin for the familiar "short range" repulsion presenting in relative terms generally between two particles at either atomic or strong or weak scale.)

Consider that relative to the CM frame not moving with the charge, similarly as the E field distribution (cf Sec 3), the charge distribution of the moving charge $\alpha = e$ or p becomes narrowed and intensified at a point transverse to its velocity, along the line joining the e, p here, which extends its rest-charge radius a^0_α by an extra distance b^0_α in the transverse direction. So the effective "radius" of the moving charge is in effect contracted from $a^0_\alpha + b^0_\alpha$. The charge space of a moving charge contracts by the same mechanism as the E field space based on the discussion above, except that a differing contraction efficiency, by a factor χ, should be allowed for the distinct charge space. Then $a_e = \frac{m_p}{M}\frac{\chi(a^0+b^0)}{\gamma}$, $a_p = \frac{m_e}{M}\frac{\chi(a^0+b^0)}{\gamma}$; $\chi > 1$ indicates a less efficient contraction for the charge. A formal relation of a and a^0 thus follows as

$$a = (a_e + a_p) + (b_e + b_p) = \frac{\chi(m_p + m_e)(a^0 + b^0)}{M\gamma} = \frac{a^0}{\gamma_a}, \quad \gamma_a = \frac{\gamma}{\chi(1 + b^0/a^0)} \tag{A.1}$$

[1] (a) Perkins DH 1982 *Introduction to High Energy Physics*, 2nd ed (Reading: Addison-Wesley); (b) Griffiths D 1987 *Introduction to elementary particles* (New York: Harper & Row); (c) Williams WSC 1992 *Nuclear and Particle Physics* (Oxford: Clarendon); (d) Enge HA 1969 *Introduction to Nuclear Physics* (Massachusetts: Addison-Wesley); (e) Beringer J, et al (Particle Data Group) 2012 *Phys. Rev.* **D86** 010001.

[2] (a) Higgs P 1964 *Phys. Lett.* **12** 132; 1964 *Phys. Rev. Lett.* **13** 508-9; *ibid* 321; Englert P and Brout R 1964 *Phys. Rev. Lett.* **13** 321; Gutranik GS, Hagen CR and Kibble TWB 1964 *Phys. Rev. Lett.* **13** 585; (b) Weinberg S 1967 *Phys. Rev. Lett.* **19** 1264; Salam A 1968 in *Elementary particle physics: relativistic groups and analicity, Nobel Symp.* **8**, Svartholm N ed (Stockholm: Almquist & Wiksells) p 367; (c) Glashow SL, Lliopoulos L and Maiani I 1970 *Phys. Rev.* **D2** 1285; (d) 'T Hooft G 1971 *Nucl. Phys.* **B33** 173-99; 1971 *Phys. Lett.* **B37** 195; (e) Fermi E 1934 *Zeit. f. Physik* **88**171; tr Wilson FL 1968 *Am. J. Phys.* **36** 1150-60.